LRP 593/97 December 1997

Feedback Stabilization of Axisymmetric Modes in the TCV Tokamak Using Active Coils Inside and Outside the Vacuum Vessel

F. Hofmann, M.J. Dutch, A. Favre, Y. Martin
J.-M. Moret, D.J. Ward

Accepted for Publication in
Nuclear Fusion

Feedback Stabilization of Axisymmetric Modes in the TCV Tokamak Using Active Coils Inside and Outside the Vacuum Vessel

F. Hofmann, M.J. Dutch, A. Favre, Y. Martin, J.-M. Moret, D.J. Ward

Centre de Recherches en Physique des Plasmas
Ecole Polytechnique Fédérale de Lausanne
Association EURATOM - Confédération Suisse
CH- 1015 Lausanne, Switzerland

Abstract:

A new vertical position control system, including an internal active coil, has become operational on TCV. The new system has made it possible to stabilize plasmas with open-loop growth rates up to 4400 sec^{-1}, currents up to 1.0 MA, and elongations up to 2.58. The closed-loop stability of the new system has been analyzed with a numerical model in which the plasma is assumed undeformable, and the power supply outputs are delayed with respect to their inputs. Model predictions agree with the main experimental results.

1. Introduction

Elongation and shaping of the plasma cross-section have become indispensable tools for improving beta limits and confinement in tokamaks. The resulting axisymmetric modes must be stabilized by a combination of passive elements and active feedback coils. Traditionally, the active coils are located outside the vacuum vessel. This is a perfectly acceptable solution if the vessel is sufficiently resistive and if the plasma cross section is only moderately elongated, or, more precisely, if the decay time of the stabilizing currents in the vacuum vessel is of the same order as the inverse growth rate of the unstable mode. On the other hand, if the vacuum vessel is highly conducting and, at the same time, the plasma elongation is high, as is the case in TCV, active stabilization from outside becomes difficult because the electrical power which is required to drive the active coils can become excessively large. Under these circumstances, it can be advantageous to stabilize the plasma from inside the vessel, since the power required to drive the internal coil is only a small fraction of that which would be necessary for an equivalent external coil. In TCV, the decay time of the m=1 vessel currents is approximately 8 ms, whereas typical inverse growth rates of axisymmetric modes are of the order of 0.3 ms. Consequently, the design of TCV includes an active internal coil.

Several tokamaks have used internal coils for improving plasma stability. On DITE [1] and JET [2], internal coil systems have been built for the purpose of actively stabilizing non-axisymmetric modes, mainly m=2, n=1. On ASDEX Upgrade, an internal passive coil is used to slow down the growth rate of the vertical instability [3]. TCV, however, is the first tokamak which routinely uses an internal active coil for feedback stabilization of axisymmetric modes.

During the first three years of its life (1993 - 1996), TCV was operated with external coils only. These coils are driven by slow, thyristor-controlled power supplies. As a result, vertical instability growth rates, elongations and plasma currents were severely limited [4]. The fast internal coil became operational in August 1996, and this paper describes the first experiments using internal and external coils jointly for feedback stabilization of the vertical instability. We also present a new model for analyzing closed-loop stabilty and we compare model predictions with experimental results.

2. Growth Rates of Axisymmetric Modes in TCV

One of the conditions that must be satisfied in a successful feedback control system is that the response time of the active coil, Δt, must be less than the inverse open-loop growth rate, γ^{-1}, of the mode to be stabilized [5]. Therefore, a precise knowledge of the axisymmetric growth rate to be expected for various plasma parameters is important for deciding on whether a particular plasma scenario is feasible or not. In TCV, open-loop growth rates have been experimentally measured for a variety of shapes and elongations [6]. These measurements were performed by opening the vertical and radial feedback control loops, during quasi-stationary conditions, and observing the exponential growth of the vertical displacement via the magnetic

and soft X ray diagnostics. Growth rates have also been computed numerically, using the NOVA-W code, and excellent agreement with measured values was found [7]. The results show that the open-loop growth rate of the vertical instability depends primarily on plasma elongation but also on a number of other parameters, such as triangularity, square-ness, vertical position within the vessel, plasma wall distance, internal inductance, poloidal beta, etc. If these other parameters are optimized to give the minimum growth rate for a given elongation, and if we assume Ohmic current profiles and low beta ($\beta_{tor} \approx 2\%$), we can express the growth rate of the vertical instability as a function of elongation and normalized current . Fig.1 shows contours of constant growth rate in the κ-I_N plane, based on NOWA-W calculations. κ is the vertical elongation of the plasma cross-section and I_N is the normalized current, defined as $I_N=I_p/(a*B_t)$, where I_p is the plasma current in MA, a is the horizontal minor radius in m and B_t is the toroidal magnetic field in T. We conclude from this figure that, for any given elongation, the normalized current not only has an upper limit, defined by the minimum stable q-value, but also a lower limit, given by the maximum growth rate which the feedback system is able to stabilize. In principle, the lower limit can be pushed to smaller values of I_N by making the feedback system faster, i.e., by reducing its response time, Δt. However, this cannot be pursued indefinitely, because as soon as the stability margin drops below a critical value (typically f=1.02), the system becomes extremely sensitive to small perturbations, e.g. ELMs or sawteeth. Such events can then project the plasma beyond the ideal stability limit (f=1) making feedback control impossible. The stability margin is defined here as $f=1+(1/(\gamma\tau_v))$, where γ is the open-loop growth rate and τ_v is the decay time of the stabilizing currents in the vacuum vessel. In TCV, the response time of the fast control loop is presently between 0.1 and 0.2ms so that one can expect to be able to stabilize axisymmetric modes with growth rates, $\gamma < 5000\ sec^{-1}$.

3. Experiments with External Coils Only

TCV is equipped with sixteen shaping coils, driven independently by thyristor-controlled power supplies, with a response time of approximately 1ms. Any combination of shaping coils can be used for vertical position control. In the experiments described here, four outboard shaping coils were used for vertical feedback. Depending on the vertical position of the magnetic axis, three different sets of coils were used, as shown in the Table, below

	Active Coil Set	Z_{axis} (range)	Z_{axis} (optimum)
a)	F1, F2, F5, F6	Z < -0.11m	Z= -0.23m
b)	F2, F3, F6, F7	-0.11m < Z < 0.11m	Z= 0
c)	F3, F4, F7, F8	Z > +0.11m	Z= +0.23m

Each F-coil has 36 turns and coil numbers are identified in Fig.2. Perfect orthogonality between the vertical and radial position control systems is achieved when the magnetic axis is at its optimum position, as given in the Table. For non-optimum axis positions, orthogonality is lost, but vertical and radial position control is still possible. The vertical position control loop consists of a Z^*I_p observer, based on magnetic measurements, a PD controller, a decoupling matrix which compensates the mutual inductances between coils, and four power supplies, one for each active coil [8]. Proportional and derivative gains can be varied arbitrarily. Optimization of these gains has made it possible to stabilize plasmas with open-loop growth rates up to 1000 sec^{-1} [7].

In the course of these experiments, several observations were made: For a given value of the proportional gain (P), there is a stable operating window for the derivative gain (D). At the lower limit of the D-window, the system starts to oscillate at a low frequency (20-40 Hz), whereas at the upper limit, it oscillates at high freqency (200-300Hz). For high open-loop growth rates, the D-window is quite small (± 5%). If D is set to a value close to the middle of its window, there is also a stable operating window for P. In contrast to the D-window, the P-window is relatively large (±30%). The size of the stable domain in P-D space decreases with increasing open-loop growth rate, and it shrinks to zero when the growth rate reaches approximately 1200 sec^{-1}.

4. Experiments with External and Internal Coils

The internal coil in TCV [9] is installed in the outboard corners of the vacuum vessel (Fig.2). It is insulated from the vessel by ceramic supports and protected from plasma contact by carbon tiles. The coil consists of 6 turns connected in series, 3 positive turns on the bottom and 3 negative turns on the top of the vessel. It is driven by a fast power supply, using IGBT technology [9], which is capable of producing a maximum current of 2kA and a maximum voltage of 560V with a response time of less than 0.1ms. The power supply is protected from voltage surges due to vertical disruptions by means of a crowbar device [9].

There are obviously many different ways to integrate fast and slow systems for combined action feedback. One possibility is to apply PD feedback to the fast coil and to drive the slow coils with a voltage which is proportional to the fast coil current [10,11]. In the work described here, we have chosen to use a different strategy. We leave the existing slow feedback system unchanged and, in addition, apply derivative feedback to the fast coil. The fast derivative gain, G, then becomes a third parameter to be optimized. Both of these feedback schemes will act in such a way as to maintain the time-averaged current in the fast coil close to zero. The main advantage of the second scheme is that it allows a smooth transition between feedback with slow coils only and combined action feedback.

Three experimental campaigns were undertaken to explore the limits of the new system. The first was aimed at stabilizing the highest possible open-loop growth rate. For this purpose,

plasmas with low current (I_p=250kA, B_t=1.43T), elliptical cross-section and large plasma-wall distance were created. A typical example is shown in Fig.3. We note that the elongation reaches a maximum value of 1.93 at t=1.3 sec. Both the safety factor at the 95% flux surface, q_{95}, and the internal inductance, l_i, are very high, leading to high growth rates of the vertical instability. At t=1.3 sec, the open-loop growth rate, as calculated with the NOVA-W code, is 4400 sec^{-1}, corresponding to a stability margin, f=1.028. The disturbance at t=0.91 sec is caused by a large deuterium gas puff which was injected at that time. The lower three traces on Fig.3 show the output of the Z^*I_p observer, the current in one of the four active slow coils (F6), and the fast coil current. We note that the fast coil current remains zero until t=0.24 sec, at which time the elongation has already reached a value of 1.74. In fact, this is about the maximum elongation that can be stabilized, at this high value of l_i, with the slow coils only. The RMS value of the fast coil current increases considerably towards the end of the discharge, when the elongation and the open-loop growth rate are slightly higher. The Z^*I_p observer output shows that the vertical displacement stays within a few mm.

The second campaign was designed to maximize the current of highly elongated, D-shaped plasmas. Here, it was found that the maximum normalized current, I_N, that can be stably confined increases with elongation, as expected, up to $\kappa \approx 2.3$. At higher elongation, however, I_N remains roughly constant, $I_N \approx 3$ MA m^{-1} T^{-1}. The current limit manifests itself by the appearance of non-axisymmetric modes which lead to a disruption [12]. In this campaign, loss of vertical position control due to excessive axisymmetric growth rates was not a problem since the growth rates were well within the capabilities of the feedback system. Fig.4 shows a discharge in which a maximum plasma current of 1.02 MA was reached. This discharge had an elongation of κ=2.28 and a very low safety factor, q_{95}=2.05. At higher elongation, low-q operation was no longer possible, and the minimum attainable q-value increased with elongation, consistent with I_N=const. In Fig.4, it should be noted that the relatively large excursions seen in the fast coil current at t=0.57 and t=0.95 sec are not caused by plasma displacements but are produced by high voltages applied to the nearby shaping coils, F2 and F7. A summary of this campaign is given in Fig.5, where we plot experimentally achieved values of q_{95} as a function of plasma elongation.

Finally, a third series of experiments was launched to explore the limits on elongation. This was done at a lower toroidal field, 1.0T, in order to minimize the risk of damage to the internal coil as a result of vertical disruptions. These experiments led to the successful stabilization of D-shaped plasmas with elongations up to 2.58. To our knowledge, this is the highest elongation ever reached in a tokamak with a single magnetic axis and conventional aspect ratio. The reconstructed equilibrium of such a discharge, with I_N=2.90 MA m^{-1} T^{-1} and κ=2.58 is shown in Fig.2. The open-loop growth rate of this discharge, γ=2700 sec^{-1}, can be compared with the theoretical predictions given in Fig.1. According to this figure, we would expect a growth rate of approximately 3000 sec^{-1}. The small discrepancy between these two values is due to the fact that the experimental plasma shape is slightly different from the one

assumed in the theoretical predictions. It should also be mentioned that higher elongations than the values reported here have been produced in doublets [13,14] and low-aspect-ratio tokamaks [15]. In the DIII-D tokamak, an elongation of κ=2.5 has been achieved with auxiliary power and ramping of the plasma current to broaden the current profile [16].

In each of the experimental campaigns descibed above, the three feedback gains (slow proportional gain, slow derivative gain and fast derivative gain) had to be slightly readjusted to maintain closed-loop stability for the various plasmas. In optimizing the slow gains for a given fast gain, we observed the same behaviour as was described in section 3, i.e., there is a stable island in P-D space, the size of which depends on the open-loop growth rate. In addition, the size of the stable island also depends on the value of the fast gain. Below a certain value of G, depending on the open-loop growth rate, there are no more stable points in P-D space. For higher values of G, the size of the stable domain increases with G, until an upper limit is reached. This limit is given by the onset of parasitic oscillations at high frequency (2-3 kHz), which are probably caused by a signal delay in the fast feedback loop. This problem is currently being investigated.

5. Closed-Loop Stability Analysis

5.1. Model

Closed-loop stability of elongated plasmas in TCV has been studied in the past with the NOVA-W code [17]. NOVA-W uses a sophisticated plasma model, including the effects of deformation of the eigenfunction. It was found [11] that a combination of external and internal coils can successfully stabilize TCV plasmas up to elongations of κ=3, provided that the vertical position observer is constructed according to the prescription given in [18]. These results, however, are not directly applicable to TCV because idealized power supplies, without delays, were assumed in the calculations [11]. Real power supplies have finite delays between input and output signals, and these delays are crucially important for determining closed-loop stability. Including signal delays in the NOVA-W model is not possible because delays introduce non-linearities and NOVA-W is basically a linear stability code [17]. In this paper, we therefore use a different approach. We assume the plasma to be a rigid, mass-less body and we introduce measured delays in the fast and slow control loops. The model consists of circuit equations for all active and passive elements in the system (fast coil, slow coils, vacuum vessel) and an equation describing the instantaneous vertical force equilibrium of the plasma,

$$\mathbf{V} = R\,\mathbf{I} + L\,\partial\mathbf{I}/\partial t + \mathbf{W}\,I_p\,\partial Z/\partial t \qquad (1)$$

$$0 = A\,Z\,I_p + \mathbf{Q}\cdot\mathbf{I} \qquad (2)$$

where **V** and **I** are vectors containing the voltages and currents of internal coils, external coils and vessel elements. The vacuum vessel is decomposed into 38 ring-shaped elements. R and L are the resistance and inductance matrices and Z measures the vertical displacement of the plasma. The vectors **W** and **Q** are composed of known Green's functions. The first term on the r.h.s. of eq. (2) represents the main destabilizing force due to the time-independent equilibrium field. The coefficient A is related to the open-loop growth rate and can be readily computed for a given equilibrium field and a given plasma current distribution. The voltages which are applied to the slow and fast coils can be expressed as

$$V_{S,0} = P[\Omega_1 \cdot \Psi + \Omega_2 \cdot \mathbf{B}] + D[\Omega_3 \cdot \partial\Psi/\partial t + \Omega_4 \cdot \partial\mathbf{B}/\partial t], \quad V_S(t) = V_{S,0}(t-\Delta) \tag{3}$$

$$V_{F,0} = G[\Omega_5 \cdot \partial\mathbf{B}/\partial t], \quad V_F(t) = V_{F,0}(t-\delta) \tag{4}$$

where $V_{S,0}$ and $V_{F,0}$ are the undelayed signals, V_S and V_F are delayed by the time-intervals Δ and δ, respectively, P, D and G are the feedback gains and the vectors Ω_1, Ω_2, Ω_3, Ω_4 and Ω_5 describe the vertical position observer. In TCV, typical time delays in the slow and fast control loops are Δ=1.0ms and δ=0.2ms, respectively. Ψ and **B** are fluxes and magnetic fields at the positions of the flux loops and magnetic field probes. These can be written as

$$\Psi = \lambda_1 \mathbf{I} + Z\, I_p\, \mathbf{Y}_1 \tag{5}$$

$$\mathbf{B} = \lambda_2 \mathbf{I} + Z\, I_p\, \mathbf{Y}_2 \tag{6}$$

where the matrices λ_1, λ_2 and the vectors $\mathbf{Y}_1$, $\mathbf{Y}_2$ contain known Green's functions and time-independent contributions have been suppressed. In equation (4) we have assumed that the fast derivative feedback uses B-probe signals only. This choice is motivated by the fact that the B-probes are mounted inside the TCV vacuum vessel, whereas the flux loops are located outside the vessel. Consequently, the B-probes are expected to provide a faster response to plasma motion than the flux loops. Typical observers are shown in Fig.6. Note that several B-probes and flux loops in the vicinity of the fast coil are not used in these observers. It should also be pointed out that the observers which we use, both in the experiments described above and in the numerical model, do not include the coil currents explicitly. It is clear that an ideal Z^*I_p observer must include the coil currents [18]. In TCV, however, the thyristor switching noise, seen on the coil current traces, is so large that it seriously disturbs the control loop. The omission of the coil currents in the Z^*I_p observer can easily be compensated by adding the contribution of these currents to the Z^*I_p reference signal, using precalculated currents.

The system of equations (1) to (6) represents a non-linear eigenvalue problem, which is conveniently solved by assuming an arbitrary complex eigenvalue and computing the corresponding P,D coefficients for a given value of G.

5.2. Results

Fig.7 shows the results of a typical stability analysis, using the model described above. All parameters which are used in the model (i.e. circuit parameters, equilibrium coil currents, plasma current distribution, Z^*I_p observers, power supply characteristics, etc.) are taken from an experimental TCV shot, with the exception of the slow proportional and derivative gains, P and D. The fast derivative gain, G, is also an input parameter. In the case we are considering here (TCV shot 7464 at time t=0.50sec), the fast coil was not activated, so that G=0. The model then computes the P,D values for a given closed-loop growth rate and oscillation frequency. Three domains can be distinguished in the P-D plane: a domain where unstable oscillating solutions are found, a domain with unstable exponential solutions and a domain where there are no unstable solutions. Experimental P,D values for TCV shot 7464 are also shown in Fig.7. They fall into the stable domain of the model. If we increase the open-loop growth rate by arbitrarily changing the constant A, the stable domain shrinks and it disappears for $\gamma \approx 1300$ sec^{-1}. The boundary of the stable domain represents the marginal stability line. As one moves along this boundary anti-clockwise, starting from the left side, the oscillation frequency increases continuously. This implies that the frequency is always higher on the upper part of the boundary than on the lower part, in agreement with experimental observations.

Fig.8 shows results for a case with much higher open-loop growth rate, γ=3700 sec^{-1}, using external and internal coils for feedback stabilization. Again, all parameters except P and D are taken from an experimental shot (TCV shot 13082 at time t=0.75sec). The fast derivative gain for this shot is G=71 μs. As in the previous case, the model predicts a stable island in the P-D plane (Fig.8). Experimental P,D values for shot 13082 are also shown in the figure. We note that the stable domain is quite small in this case, reflecting the fact that the open-loop growth rate is not far from the limit of the system. The effects of varying the fast gain, G, and the open-loop growth rate, γ are illustrated in Fig.9. Using the experimental value of A, we observe that stability is lost for G < 55 μs (Fig.9a). On the other hand, if we take the experimental value of G (71 μs), the stable island disappears for $\gamma > 6000$ sec^{-1} (Fig.9b).

In summary, we note that the model results described above agree with the main experimental observations as presented in sections 3 and 4. In all cases investigated so far, the experimental P,D gains fall within or very close to the stable domain of the model. This allows us to use the model for testing the feasibility of new plasma scenarios or for optimizing the Z^*I_p observer for a given plasma configuration. Model calculations can thus considerably reduce the machine-time which is usually spent in trial-and-error optimization.

6. Conclusion

The addition of an active internal coil, driven by a fast power supply, has greatly extended the stable operating domain of TCV. Higher elongations and plasma currents can now be reached and much higher open-loop growth rates can be stabilized. In particular, the active internal coil has allowed us to create plasmas with elongations up to 2.58. This is, as far as we

know, the highest elongation ever produced in a single-axis tokamak with conventional aspect ratio. Closed-loop stability analysis has shown that the main experimental observations can be reproduced fairly accurately with a relatively simple model, in which the plasma is assumed to be rigid and the power supplies are characterized by fixed time-delays between input and output.

Acknowledgements

It is a pleasure to acknowledge the competent support of the entire TCV team. This work was partly supported by the Fonds National Suisse de la Recherche Scientifique.

References

[1] Morris, A.W., et al., Phys. Rev. Lett. **64** (1990) 1254.

[2] Santagiustina, A., et al., in Fusion Technology 1996 (Proc. 19th Symp. Lisbon, 1996), Elsevier, Amsterdam and New York (1997) 989.

[3] Köppendörfer, W., et al., in Plasma Physics and Controlled Fusion Research 1992 (Proc. 14th Int. Conf. Würzburg, 1992), Vol. 1, IAEA (1992) 127.

[4] Hofmann, F. et al., Plasma Phys. Control. Fusion **36** (1994) B277.

[5] Noll, P. et al., in Controlled Fusion and Plasma Heating (Proc. 17th Europ. Conf. Amsterdam, 1990), Vol. 14B, Part I, European Physical Society, Geneva (1990) 419.

[6] Dutch, M.J., et al. in Controlled Fusion and Plasma Physics (Proc. 22nd Eur. Conf. Bournemouth, 1995), Vol. 19C, Part IV, European Physical Society, (1995) 77.

[7] Hofmann, F. et al., Nuclear Fusion **37** (1997) 681.

[8] Lister, J.B., et al. Fusion Technology **32** (1997) 321.

[9] Favre, A., et al., in Fusion Technology 1996 (Proc. 19th Symp. Lisbon, 1996), Elsevier, Amsterdam and New York (1997) 1107.

[10] Marcus, F.B., et al., Nuclear Fusion **30** (1990) 1511.

[11] Ward, D.J., et al., Nuclear Fusion **34** (1994) 401.

[12] Hofmann, F., et al., in Controlled Fusion and Plasma Physics (Proc. 24nd Eur. Conf. Berchtesgaden, 1997), Vol. 21A, Part II, European Physical Society, (1997) 525.

[13] Ohkawa, T., et al., in Plasma Physics and Controlled Fusion Research 1974 (Proc. 5th Int. Conf. Tokyo, 1974), Vol. 1, IAEA (1975) 281.

[14] Wesley, J.C., et al., in Plasma Physics and Controlled Fusion Research 1980 (Proc. 8th Int. Conf. Brussels, 1980), Vol. 1, IAEA (1981) 35.

[15] Sykes, A., Plasma Phys. Control. Fusion **36** (1994) B93.

[16] Taylor, T.S., et al., in Plasma Physics and Controlled Fusion Research 1990 (Proc. 13th Int. Conf. Washington, D.C., 1990), Vol. 1, IAEA (1991) 177.

[17] Ward. D.J. et al., J. Comput. Phys. **104** (1993) 221.

[18] Hofmann, F., Jardin, S.C., Nuclear Fusion **30** (1990) 2013.

Figure Captions

Fig.1. Open-loop growth rate of the vertical instability (in sec^{-1}) of D-shaped plasmas in TCV, calculated with the NOVA-W code, as a function of elongation and normalized current.

Fig.2. Reconstructed equilibrium of TCV-shot 12868, at t=0.725 sec. Plasma parameters: I_p=726kA, B_t=1.0T, κ=2.58, q_{95}=2.62, γ=2700 sec^{-1}. Feedback gains: P=0.039, D=0.24ms, G=88μs.

Fig.3. TCV-shot 13082 with maximum growth rate of the vertical instability. Plasma parameters at t=1.3 sec: I_p=250kA, B_t=1.43T, κ=1.93, q_{95}=5.5, γ=4400 sec^{-1}. Feedback gains: P=0.034, D=0.18ms, G=71μs. Currents are in A, Z^*I_p is in Am.

Fig.4. TCV-shot 11368, with maximum plasma current. Plasma parameters at t=0.65 sec: I_p=1.027MA, B_t=1.43T, κ=2.28, q_{95}=2.05, γ=1200 sec^{-1}. Feedback gains: P=0.031, D=0.25ms, G=106μs. Currents are in A, Z^*I_p is in Am.

Fig.5. Experimentally achieved values of q_{95} vs. elongation for D-shaped plasmas in TCV.

Fig.6. Vertical position observer used in shot 13082. (a) flux loop coefficients, (b) magnetic field probe coefficients. Flux loops and magnetic field probes are mounted directly on the wall of the vacuum vessel, roughly equidistant in the poloidal plane. Loops are outside and probes are inside the vessel. They are numbered clockwise, starting from the inboard midplane. For shot 13082, $\Omega_3 = \Omega_1$ and $\Omega_2 = \Omega_4 = \Omega_5$.

Fig.7. Closed-loop stability analysis of shot 7464 at t=0.50 sec, using slow coils only for vertical position control. Unstable oscillatory solutions (+), unstable exponential solutions ($\Diamond$) and the experimental point ($\Box$) are shown.

Fig.8. Closed-loop stability analysis of shot 13082 at t=0.75 sec, using slow and fast coils for vertical position control. Unstable oscillatory solutions (+), unstable exponential solutions ($\Diamond$) and the experimental point ($\Box$) are shown.

Fig.9a. Marginal stability lines for four values of the fast derivative gain, G=55 μs (+), G=61 μs ($\Diamond$), G=68 μs (Δ) and G=74 μs ($\Box$). The open-loop growth rate is fixed, γ=3700 sec^{-1}.

Fig.9b. Marginal stability lines for six values of the open-loop growth rate, γ=3333 sec^{-1} ($\ast$), γ=3703 sec^{-1} ($\times$), γ=4166 sec^{-1} ($\square$), γ=4762 sec^{-1} (Δ), γ=5555 sec^{-1} ($\Diamond$) and γ=6666 sec^{-1} (+). The fast derivative gain is fixed, G=71 μs.

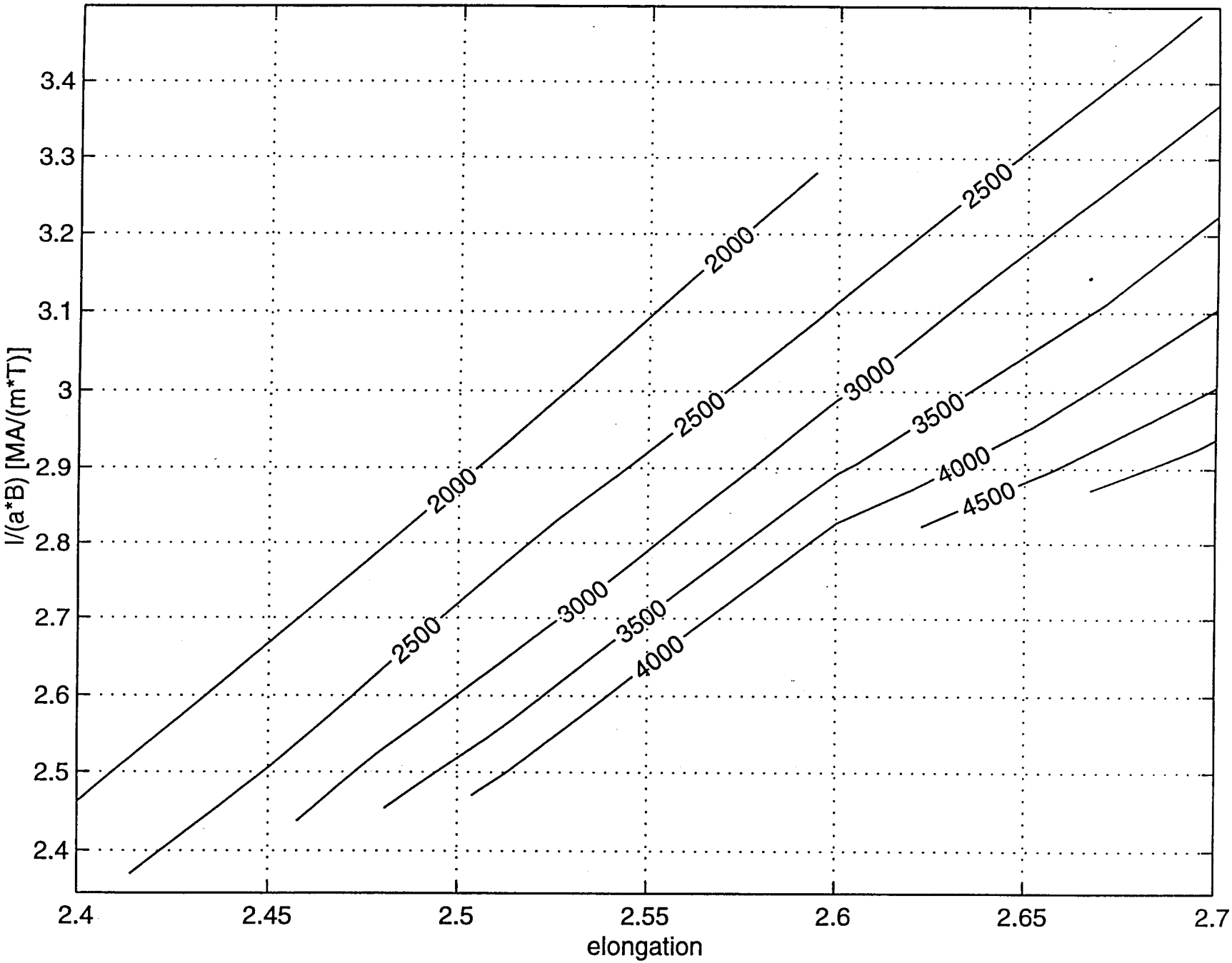
I/(a*B) [MA/(m*T)]
elongation
3.4
3.3
3.2
3.1
3
2.9
2.8
2.7
2.6
2.5
2.4
2.4
2.45
2.5
2.55
2.6
2.65
2.7
2000
2500
3000
3500
4000
4500
2000
2500
3000
3500
4000
2500

Fig.1.

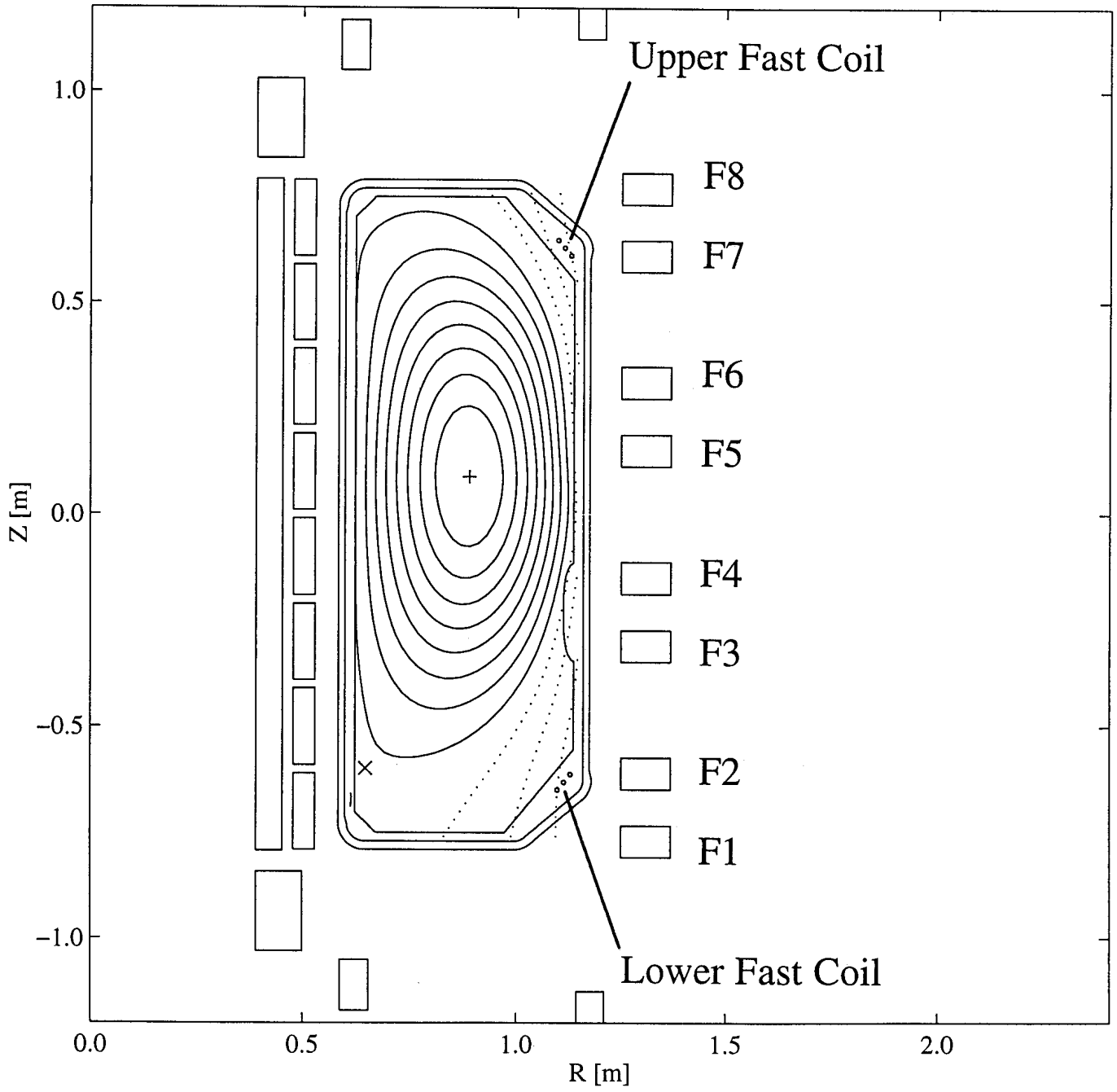
Upper Fast Coil
F8
F7
F6
F5
F4
F3
F2
F1
Lower Fast Coil
1.0
0.5
0.0
−0.5
−1.0
Z [m]
0.0
0.5
1.0
1.5
2.0
R [m]

Fig.2.

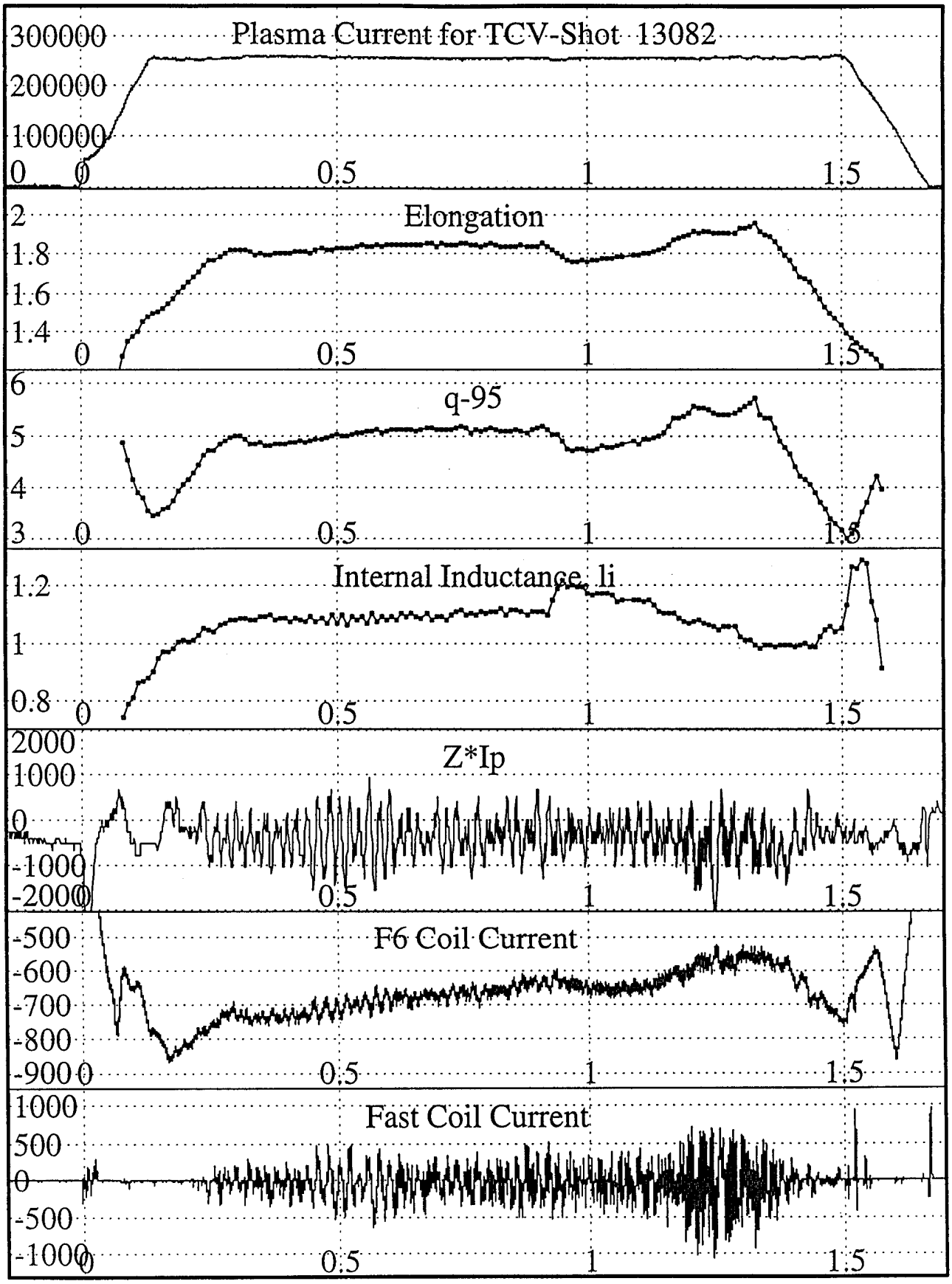
Plasma Current for TCV-Shot 13082
300000
200000
100000
0
0
0.5
1
1.5
Elongation
2
1.8
1.6
1.4
0
0.5
1
1.5
q-95
6
5
4
3
0
0.5
1
1.5
Internal Inductance, li
1.2
1
0.8
0
0.5
1
1.5
Z*Ip
2000
1000
0
-1000
-2000
0.5
1
1.5
F6 Coil Current
-500
-600
-700
-800
-900
0
0.5
1
1.5
Fast Coil Current
1000
500
0
-500
-1000
0
0.5
1
1.5
Time (sec)

Fig.3.

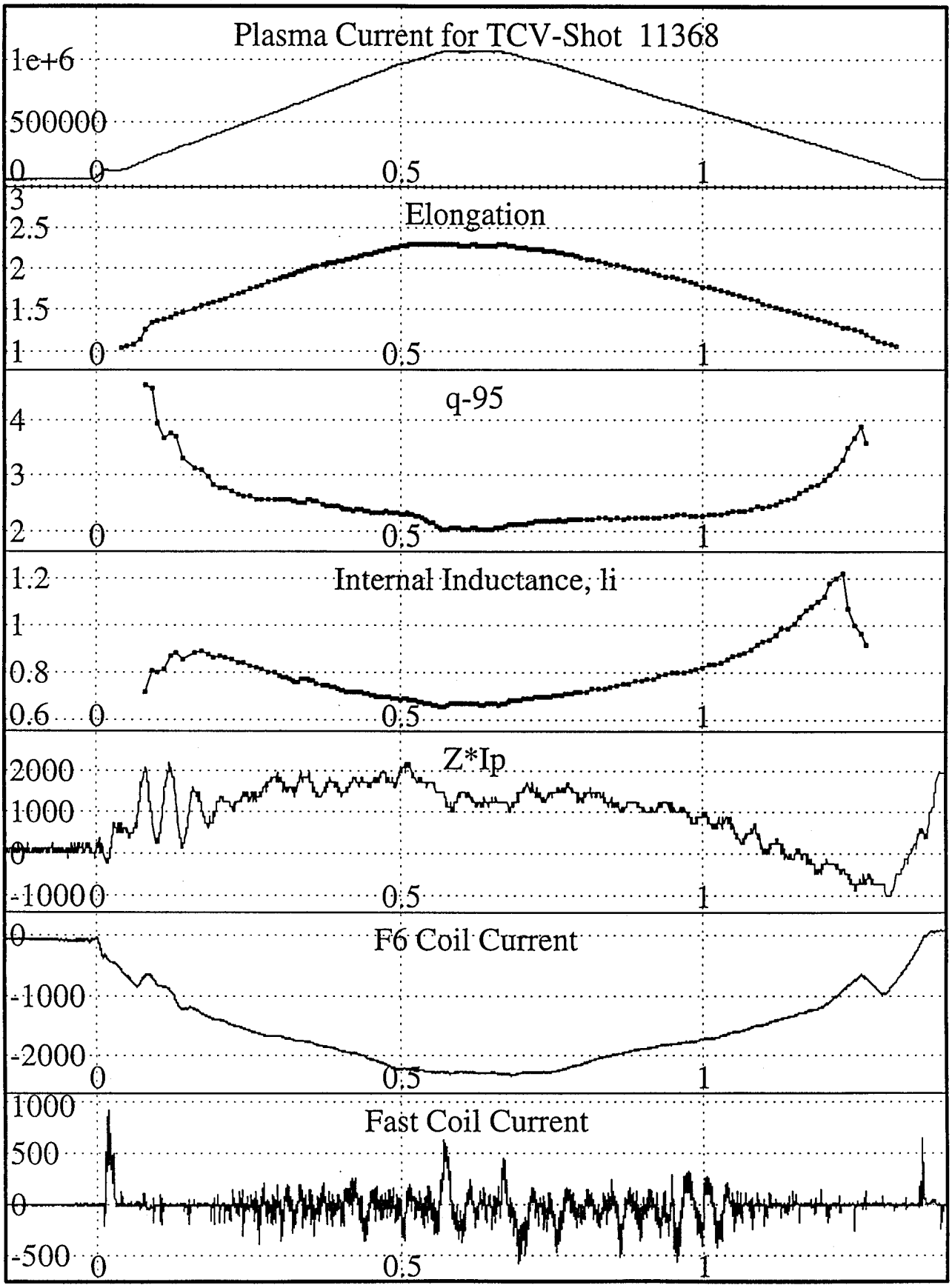
Plasma Current for TCV-Shot 11368
1e+6
500000
0
0
0.5
1
Elongation
3
2.5
2
1.5
1
0
0.5
1
q-95
4
3
2
0
0.5
1
Internal Inductance, li
1.2
1
0.8
0.6
0
0.5
1
Z*Ip
2000
1000
0
-1000
0
0.5
1
F6 Coil Current
0
-1000
-2000
0
0.5
1
Fast Coil Current
1000
500
0
-500
0
0.5
1
Time (sec)

Fig.4.

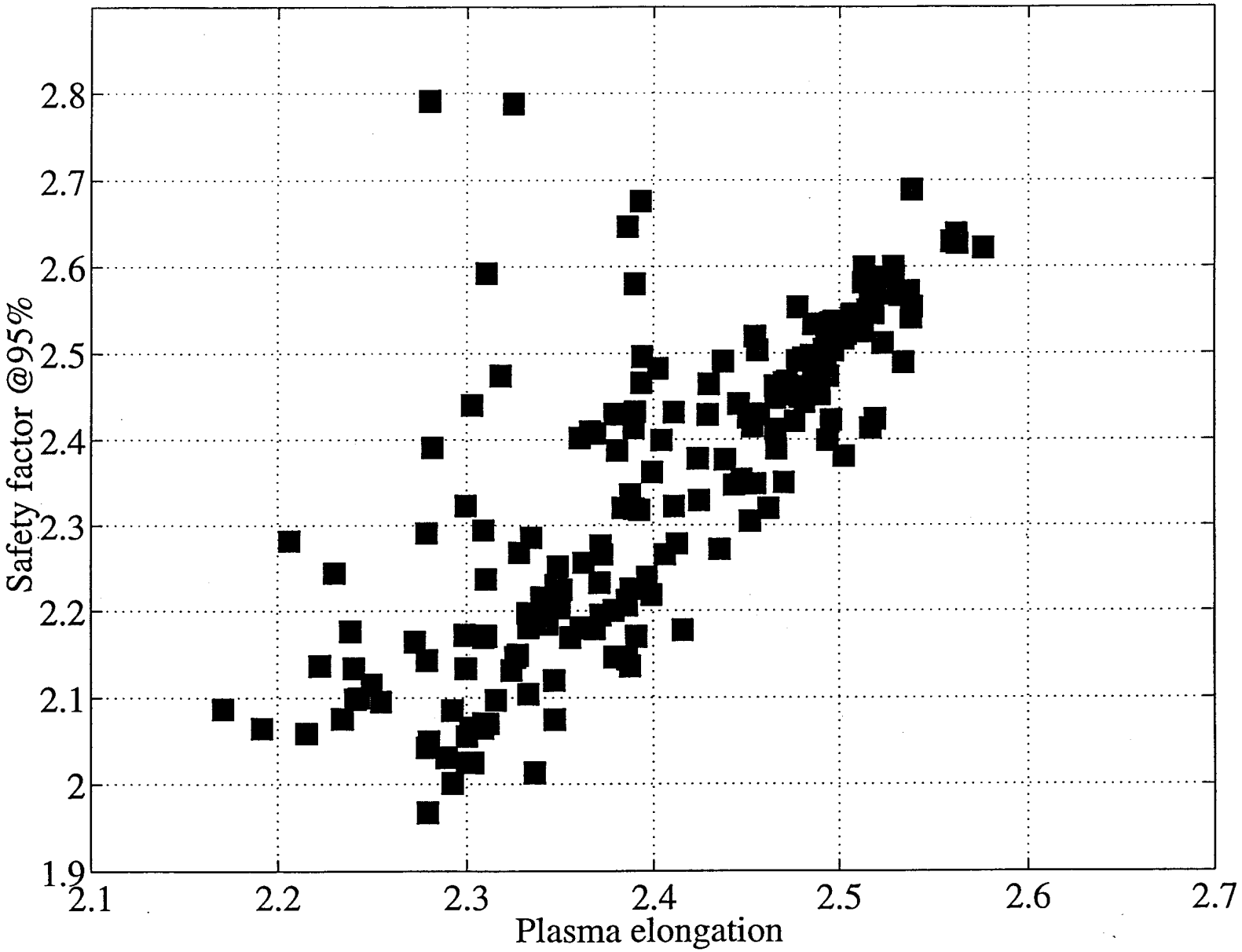
Safety factor @95%
2.8
2.7
2.6
2.5
2.4
2.3
2.2
2.1
2
1.9
2.1
2.2
2.3
2.4
2.5
2.6
2.7
Plasma elongation

Fig.5.

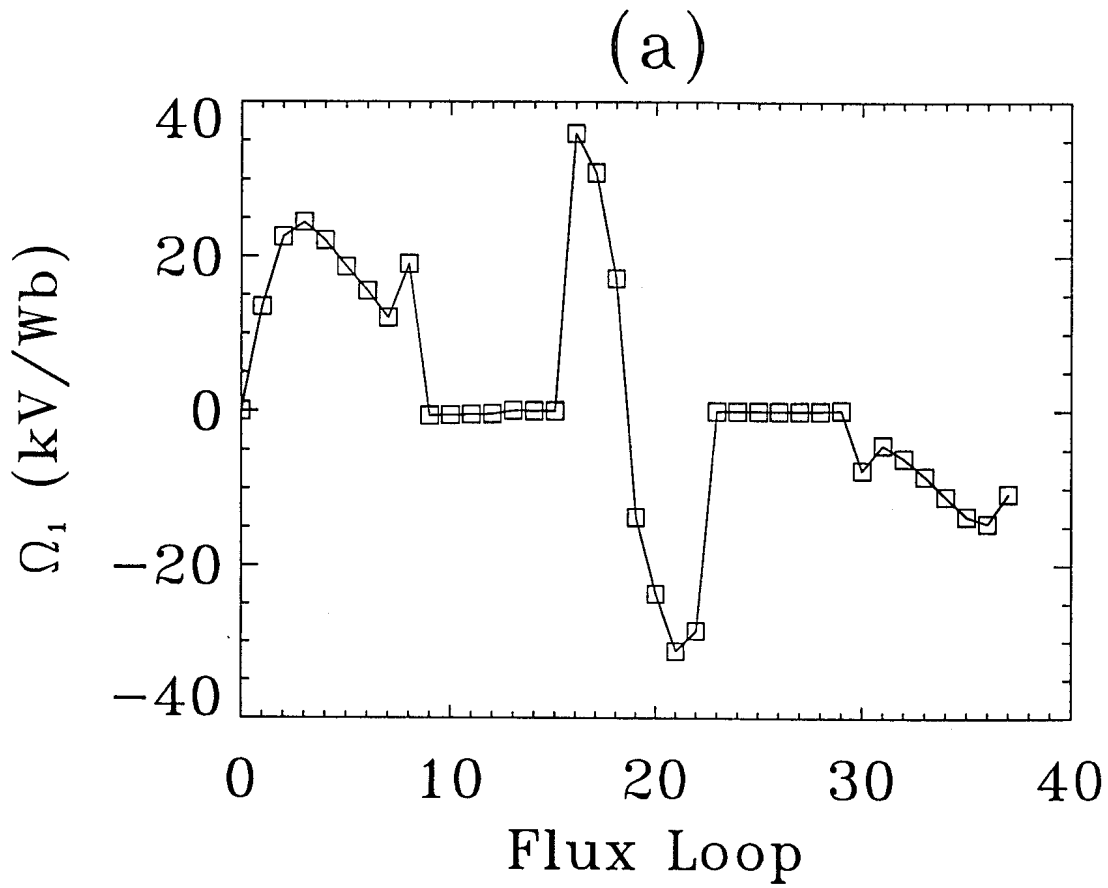
(a)
40
20
0
−20
−40
Ω_1 (kV/Wb)
0
10
20
30
40
Flux Loop

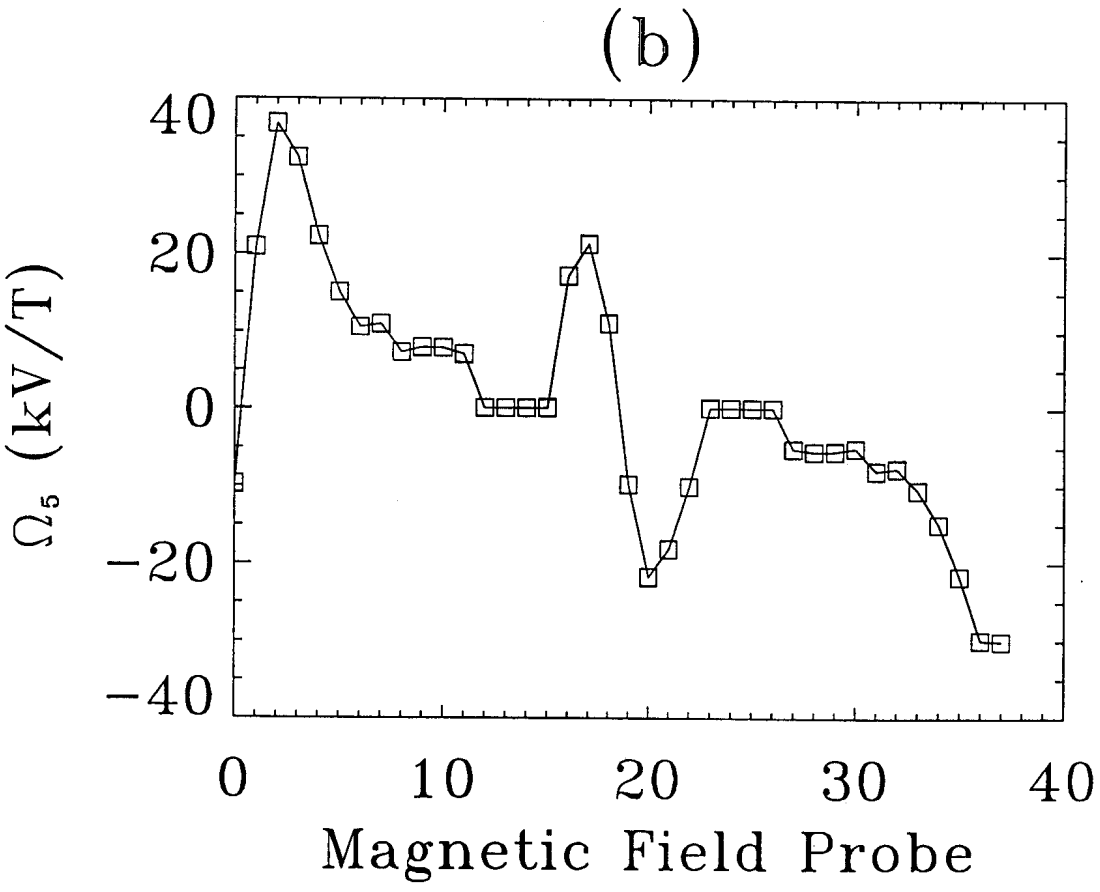
(b)
40
20
0
−20
−40
Ω_5 (kV/T)
0
10
20
30
40
Magnetic Field Probe

Fig.6.

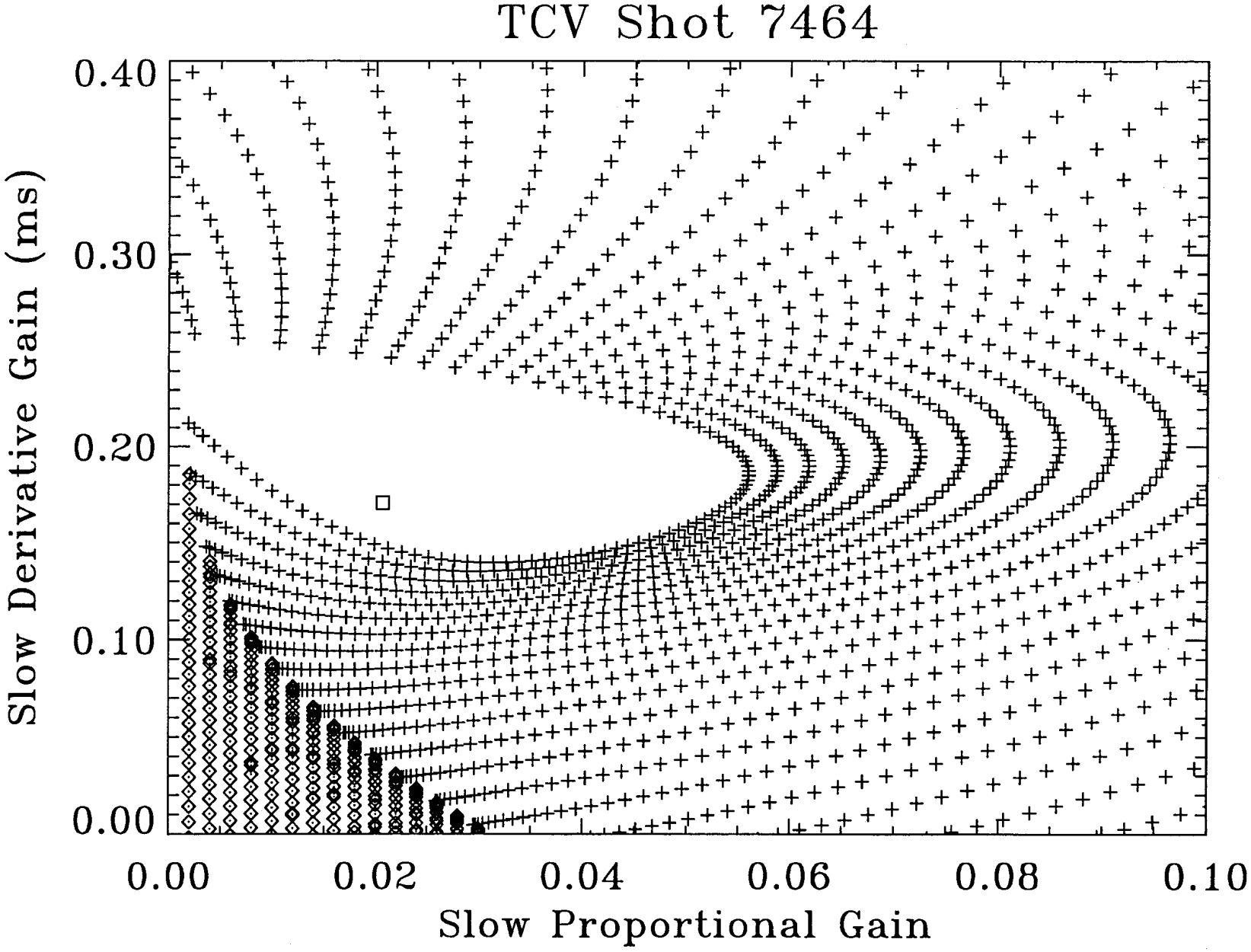
TCV Shot 7464
Slow Derivative Gain (ms)
0.40
0.30
0.20
0.10
0.00
0.00
0.02
0.04
0.06
0.08
0.10
Slow Proportional Gain

Fig.7

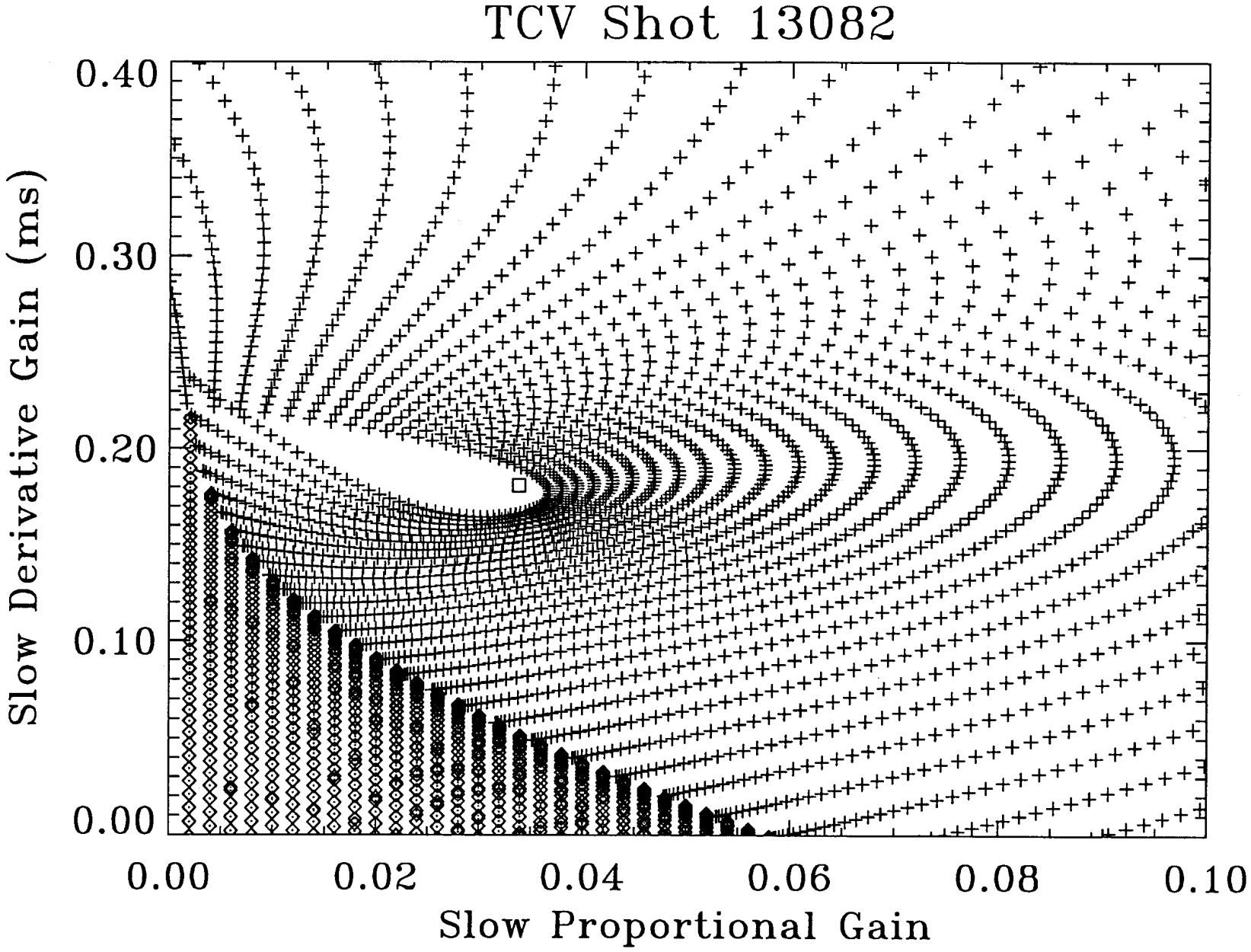
TCV Shot 13082
Slow Derivative Gain (ms)
0.40
0.30
0.20
0.10
0.00
0.00
0.02
0.04
0.06
0.08
0.10
Slow Proportional Gain

Fig.8.

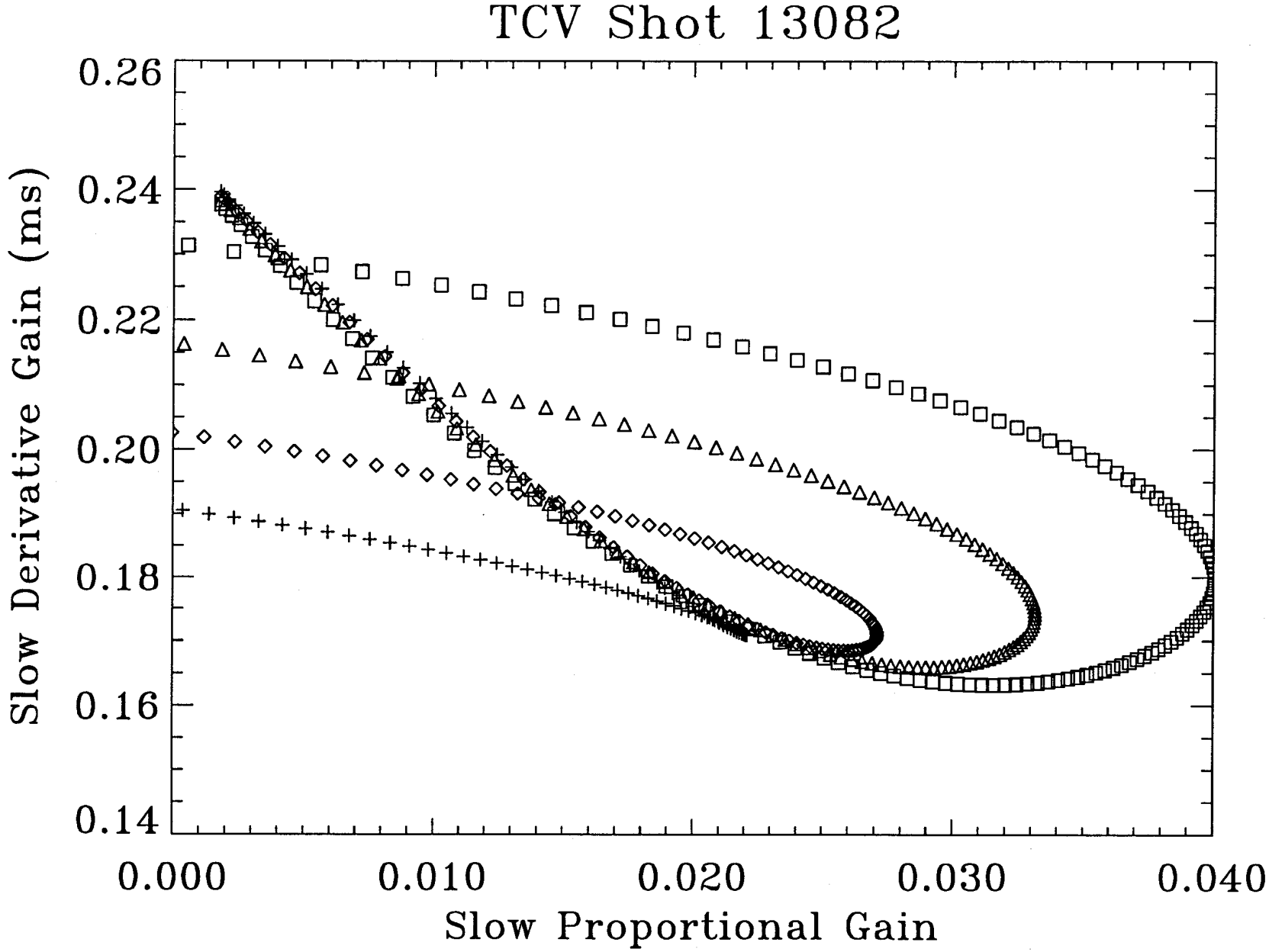
TCV Shot 13082
Slow Derivative Gain (ms)
0.26
0.24
0.22
0.20
0.18
0.16
0.14
0.000
0.010
0.020
0.030
0.040
Slow Proportional Gain

Fig.9a.

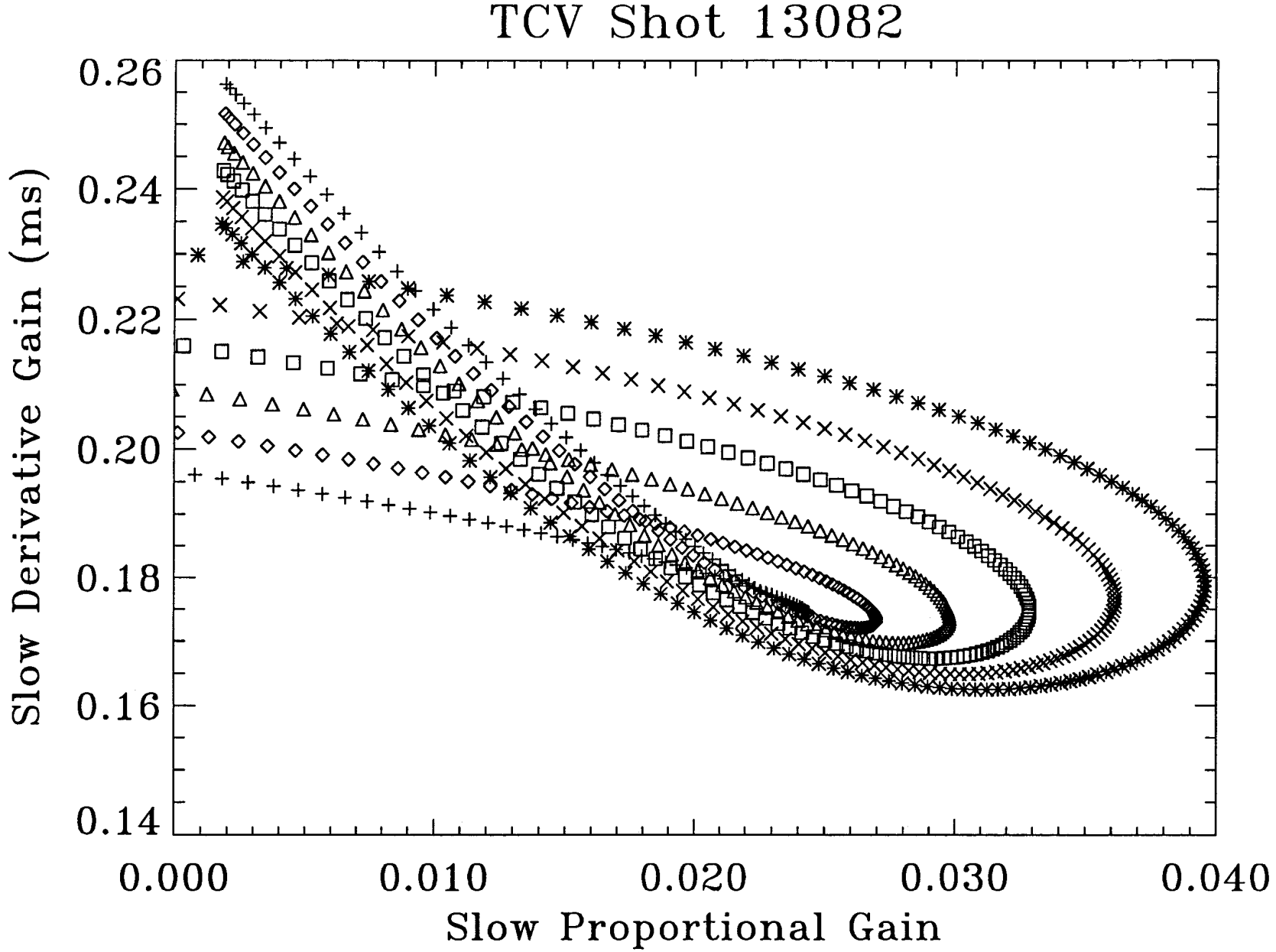
TCV Shot 13082
Slow Derivative Gain (ms)
0.26
0.24
0.22
0.20
0.18
0.16
0.14
0.000
0.010
0.020
0.030
0.040
Slow Proportional Gain

Fig.9b.